Establishment of a Comprehensive Drought Monitoring Index Based on Multisource Remote Sensing Data and Agricultural Drought Monitoring

Zhaoxu Zhang, Wei Xu, Zhenwei Shi, and Qiming Qin

***Abstract*—The occurrence of drought is a complex process and is caused by the interaction of multiple drought-causing factors. The construction of traditional drought models and indexes seldom considers multiple drought-causing factors. This study integrated the precipitation, soil water and heat balance, and crop growth during drought. From the beginning of the process of agricultural drought, the atmosphere, soil, and crops that characterize drought are considered, through the principal component analysis method to construct a comprehensive drought monitoring index (CDMI). This index was verified by using the areas covered by drought, areas affected by drought, relative soil moisture, and crop yield. The annual average CDMI had negative correlations with areas covered and affected by drought. The correlation coefficients were –0.68 and –0.73. Moreover, the CDMI value had positive correlations with relative soil moisture and crop yield. The maximum correlation coefficient between CDMI and relative soil moisture was 0.91, and the correlation coefficient with maize yield was 0.52. Subsequently, the CDMI was applied to long-term drought monitoring in agricultural areas during the summer maize growing season (June to September) in Henan Province. Results showed that the most severe years of agricultural drought in Henan Province were 2000, 2001, 2004, 2006, 2008, and 2014. The most severe agricultural drought occurred in July and August 2014. Statistics found that Henan Province had high frequencies of severe drought. This study proved that CDMI calculated by multisource remote sensing data is a reliable and effective indicator for monitoring and assessing agricultural drought.**

***Index Terms*—Agricultural drought, index, multi-source data, remote sensing.**

I. Introduction

DROUGHT is a frequent and potential continuous natural phenomenon that directly affects social and economic development, industrial and agricultural production, urban and rural water supply, people's lives, and the ecological environment [1]–[5]. The occurrence of drought can last a long time and is very destructive. Hence, drought monitoring has received considerable attention from scholars [6], [7]. Recently, drought has become a global concern [7]. Considering the complexity of drought, accurately defining drought is difficult [7]. Currently, drought is generally divided into meteorological, hydrological, agricultural, and socio-economic drought [6], [8]–[10]. Among them, agricultural drought means that during the growth of crops, soil moisture cannot meet the water requirements for normal crop growth, resulting in reduced crop yields [11].

The methods of drought monitoring mainly include two types. One is through actual site-based data, and the other is based on remote sensing data [8]. Historically, the drought monitoring method is mainly based on precipitation and air temperature measured at stations [12]. The most widely used drought indexes based on site data include standardized precipitation index (SPI) [13], palmer drought severity index [14], and standardized precipitation evapotranspiration index (SPEI) [15]. The site-based data can be used to obtain long-term drought monitoring distribution data. However, some stations are sparsely distributed at the regional scale, and observing the information of soil and vegetation using site-based data is difficult [16]–[18]. Remote sensing can obtain real-time data with information coming from the atmosphere, soil, and vegetation. The agricultural drought indexes established based on remote sensing methods are greatly suitable for long-term drought monitoring [18]. The drought indexes established based on a single data source include following: the normalized difference vegetation index (NDVI) [19], [20], vegetation condition index (VCI) [21]–[23], temperature condition index (TCI) based on land surface temperature (LST) [21]–[23], precipitation condition index (PCI) based on microwave precipitation data [24], soil moisture condition index (SMCI) based on soil moisture [25], and others. Recently, researchers have improved the timeliness and accuracy of drought monitoring by integrating a variety of remote sensing data to construct new drought indexes. Among them, vegetation health index (VHI) [23], which combines the characteristics of VCI and TCI, is more conducive to regional agricultural drought monitoring. However, using VHI should be undertaken with caution in humid areas at high latitudes, vegetation growth is restricted by lower temperatures in these areas [26]. Using precipitation data from tropical rainfall measuring mission (TRMM), some comprehensive drought indexes were established by combining TCI, VCI, and PCI, which enables the monitoring of meteorological and agricultural drought conditions. The scaled drought

Manuscript received October 6, 2020; revised December 21, 2020 and January 8, 2021; accepted January 13, 2021. Date of publication January 15, 2021; date of current version February 3, 2021. This work was supported in part by the National Natural Science Foundation of China under Grant 41771371 and in part by the National Key Technologies Research and Development Program of China under Grant 2016YFD0300603. *(Corresponding author: Qiming Qin.)*

Zhaoxu Zhang, Wei Xu, and Zhenwei Shi are with the School of Earth and Space Sciences, Peking University, Beijing 100871, China (e-mail: zhaoxuzhang@pku.edu.cn; xuwei1995@pku.edu.cn; zwshi@pku.edu.cn).

Qiming Qin is with the School of Earth and Space Sciences, Peking University, Beijing 100871, China, and also with the Geographic Information System Technology Innovation Center, Ministry of Natural Resources, Beijing 100812, China (e-mail: qmqin@pku.edu.cn).

Digital Object Identifier 10.1109/JSTARS.2021.3052194

condition index (SDCI) was constructed using three indicators (TCI, VCI, and PCI) in different percentages to monitor agricultural drought in North and South Carolina, United States [24]. The synthesized drought index (SDI) is defined as the main components of VCI, TCI, and PCI and is used to monitor the comprehensive drought in Shandong Province, China [27]. SDCI and SDI does not consider the effects of soil moisture which is an important characteristic parameter of drought. The microwave integrated drought index is developed by using multisensor microwave indexes (TCI, SMCI, and PCI) to monitor the distribution of short-term drought in North China [25]. The optimized meteorological drought index (OMDI) and the optimized vegetation drought index (OVDI) are established from multisource satellite data to monitor comprehensive information of drought from meteorological and agricultural aspects [28]. OMDI and OVDI lack consideration of distinctions of seasons and the correlations between satellite indexes. Drought is a complex process, and establishing agricultural drought monitoring indexes by using multisource data has become a trend [8], [12].

The occurrence of agricultural drought is a process that includes the comprehensive effects of atmosphere, soil, and crops [29]. Moreover, the occurrence of meteorological drought, which is caused by insufficient precipitation, often leads to agricultural drought. When meteorological drought occurs, the water and heat balance of soil and crops will change. Research of agricultural drought focuses on farmland and crops, in which soil moisture plays a vital role. When the precipitation is insufficient, the soil moisture content decreases. In the early stage of agricultural drought, soil moisture deficiency will lead to reduced soil evapotranspiration. Then crops cannot absorb enough water to compensate for leaf transpiration, and crop water demand and soil water supply are unbalanced, resulting in increased soil and canopy temperature [30]. When the drought continues, the physiological growth of crops is under stress, and its growth process changes. The lack of water in crops will hinder crop photosynthesis and material metabolism. When crops are continuously exposed to water stress, their stomata will close, which affects photosynthesis and changes the chlorophyll fluorescence value. When crops begin to wither, the reflectivity of the crop's sensitive waveband will have changes [31]. If the water shortage reaches a serious state, then crops will eventually die, resulting in reduced crop yields [32]. Hence, understanding the process of agricultural drought is of positive significance for the construction of the agricultural drought monitoring index.

Drought is a slow and long-term process. First, it starts with insufficient precipitation, leading to soil moisture deficit, and then the surface temperature rises, which will eventually affect the yield of crops. Most agricultural drought indices are based on linear models. However, agricultural drought does not have a linear relation with VI, LST, precipitation, soil moisture anomalies in different time and regions. There exist correlations between those factors that characterize drought. As a linear change method, principal component analysis (PCA) method can reduce redundancy of information. This study comprehensively considered the factors that characterized the occurrence of agricultural drought, such as the atmosphere, soil, and crops. Not only the influence of precipitation, NDVI, and LST on drought are considered, but also the information of microwave soil moisture, evapotranspiration and solar-induced chlorophyll fluorescence (SIF). This study aims the following.

1) Establish a comprehensive drought monitoring index (CDMI) from multisource remote sensing data.
2) Use areas covered by drought, areas affected by drought, relative soil moisture, and maize yield to verify CDMI.
3) Monitor and assess long-term agricultural drought in agricultural areas of Henan Province from 2000 to 2018.

II. Study Area and Data

A. Study Area

The research area is located in Henan Province, China, and extends from 31°23′N-36°22′N, 110°21′E-116°39′E [5]. Fig. 1 shows the land use types in this study area. Henan Province is a transitional climate between subtropical humid and warm temperate semi-humid monsoon climate, with an average annual precipitation of 500–900 mm. Henan is a major food province where maize is the main crop in summer [33]. The growing season of summer maize is from June to September.

B. Data

1) Vegetation Index Data: NDVI is one of the most widely used agricultural drought monitoring indices, which can be calculated from near-infrared and red-light bands. Moderate Resolution Imaging Spectroradiometer (MODIS) provides monthly NDVI products with 1 km spatial resolution. The monthly NDVI (MOD13A3) data were downloaded from 2000 to 2018.[1]

2) Land Surface Temperature Data: MODIS provides 8-day LST products (day and night) with a spatial resolution of 1 km. The day and night products of MODIS LST (MOD11A2) from 2000 to 2018 were downloaded, and the monthly LST results were calculated by the maximum value synthesis method.

3) Evapotranspiration Data: Evapotranspiration (ET) can reflect the quality and energy exchange of soil, vegetation, and atmosphere. The actual ET (ETa) is generated using the simplified surface energy balance (SSEBop) model [34]. The monthly evapotranspiration data with a spatial resolution of $0.25 * 0.25°$ were downloaded.[2]

4) Meteorological Data: The monthly TRMM precipitation data (3B43) were obtained from the Goddard Earth Sciences Data and Information Services Center.[3] The spatial resolution of precipitation data is $0.25 \times 0.25°$.

To analyze the meteorological drought in Henan Province, the SPEI-01 data were obtained from 2000 to 2018.[4]

5) Soil Moisture Data: Soil moisture (SM) is an important parameter for agricultural drought. The daily soil moisture data were obtained from the European Space Agency (ESA CCI)

[1][Online]. Available: https://ladsweb.nascom.nasa.gov/search
[2][Online]. Available: https://github.com/zhangfeng0826/ETdata
[3][Online]. Available: http://disc.sci.gsfc.nasa.gov/
[4][Online]. Available: https://spei.csic.es/

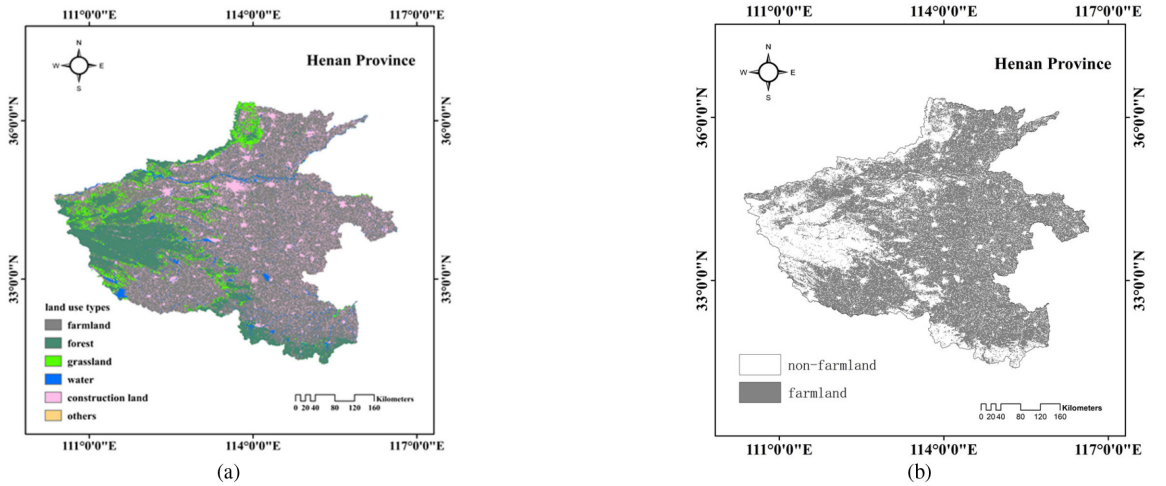

Fig. 1. Land use types map in Henan Province, China. (a) land use map and (b) agricultural areas map.

from 2000 to 2018.[5] The monthly soil moisture results were calculated by the maximum value synthesis method.

6) Solar-Induced Chlorophyll Fluorescence Data: A new global solar-induced chlorophyll fluorescence (GOSIF) dataset with high spatiotemporal resolution (0.05°, 8-day and monthly) was developed by Li and Xiao (2019) using the data-driven method [35].[6] The monthly SIF data during maize growing season were downloaded.

7) Other Data:

a) Land use data: The land use data with a spatial resolution of 1 km used in this study was obtained from the Resource and Environment Science and Data Center.[7] Land use types include farmland, forest, grassland, water, construction land, and others [see Fig. 1(a)]. Farmland is the research object in this study. Therefore, based on land-use data, the farmland was extracted to monitor agricultural drought [see Fig. 1(b)].

b) Site-based data: Relative soil moisture is a direct indicator of agricultural drought. The 10 cm relative soil moisture data were downloaded through the China Meteorological Data Network.[8] Every 10-day data were provided by this website from 1991 to 2009, the monthly site-based data were obtained by averaging data from upper, middle and late 10-day.

c) Statistical data: The annual areas covered by drought, areas affected by drought, and annual regional level summer maize yield data were obtained from the National Bureau of Statistics of the People's Republic of China.[9] The areas covered and affected by drought are statistical data and can characterize the extent of the impact of drought. The drought affected crop area is more appropriate to assess the drought effect on agriculture.

In this study, due to the different resolutions and projections of multi-source remote sensing datasets, the monthly products were spatially resampled onto a 0.00834° (about 1 km) geographic Climate Modelling Grid under a World Geodetic System -1984 Coordinate System (WGS-84) geographic coordinate system.

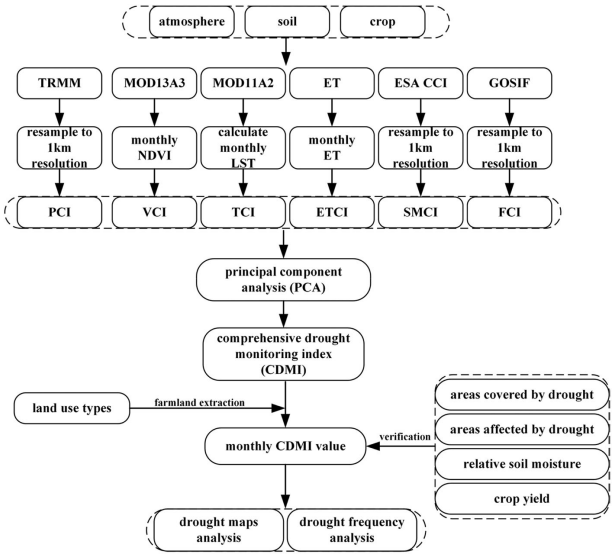

Fig. 2. Flowchart of this study.

III. Method

Agricultural drought is usually caused by insufficient precipitation for a long time, and the soil moisture cannot meet the water demand for crop growth. Agricultural drought is the result of the combined effects of the atmosphere, soil, and crops. Therefore, this study considered multiple drought-causing factors when constructing the CDMI. This study combined six indexes [PCI, VCI, TCI, SMCI, evapotranspiration condition index (ETCI), and fluorescence condition index (FCI)] using the PCA method to calculate the CDMI. Fig. 2 shows the specific process.

A. Normalized Remote Sensing Data

1) VCI: The impact of agricultural drought on crops is difficult to detect directly by NDVI [36], [37]. The VCI calculated

[5][Online]. Available: http://www.esa-cci.org
[6]The GOSIF data are available online at http://globalecology.unh.edu
[7][Online]. Available: http://www.resdc.cn/
[8][Online]. Available: http://data.cma.cn
[9][Online]. Available: http://www.stats.gov.cn/

based on NDVI can monitor local differences in ecosystem productivity [21]. VCI can better reflect the impact of drought stress on vegetation. The definition of VCI is as follows:

$$\mathrm{VCI} = \frac{\mathrm{NDVI} - \mathrm{NDVI}_{\min}}{\mathrm{NDVI}_{\max} - \mathrm{NDVI}_{\min}} \tag{1}$$

where NDVI, $\mathrm{NDVI}_{\max}$, and $\mathrm{NDVI}_{\min}$ are the values of NDVI, maximum NDVI, and minimum NDVI of each pixel, respectively, in the same month during the study period of 2000–2018. VCI changes from 0 to 1, and the corresponding vegetation conditions change from extremely low to optimal.

2) TCI: TCI is a drought monitoring index calculated based on LST, which is used to determine temperature-related drought phenomena [22]. When the drought occurs, the soil moisture decreases, causing temperature to change. High temperature during the crops growing season reflects drought. TCI is defined as follows:

$$\mathrm{TCI} = \frac{\mathrm{LST}_{\max} - \mathrm{LST}}{\mathrm{LST}_{\max} - \mathrm{LST}_{\min}} \tag{2}$$

where TCI, $\mathrm{TCI}_{\max}$, and $\mathrm{TCI}_{\min}$ are the values of TCI, maximum TCI, and minimum TCI of each pixel, respectively, in the same month during the study period of 2000–2018. Under drought conditions, TCI is close or equal to 0; and under humid conditions, TCI is close to 1. The monthly TCI dataset was established of Henan Province from 2000 to 2018.

3) ETCI: ET is very important indicator for agriculture and water resources monitoring [38]. To monitor crop water deficit and agricultural drought, ETCI is defined as follows:

$$\mathrm{ETCI} = \frac{\mathrm{ET}_{\max} - \mathrm{ET}}{\mathrm{ET}_{\max} - \mathrm{ET}_{\min}} \tag{3}$$

where ET, $\mathrm{ET}_{\max}$, and $\mathrm{ET}_{\min}$ are the values of ET, maximum ET, and minimum ET of each pixel, respectively, in the same month during the study period of 2000–2018. ETCI changed from 0 to 1, corresponding to the change of agricultural drought.

4) PCI: PCI is an index that can provide meteorological drought information, and agricultural drought is often caused by meteorological drought [39]. TRMM 3B43 can provide estimates of monthly precipitation. PCI is defined as follows:

$$\mathrm{PCI} = \frac{\mathrm{TRMM} - \mathrm{TRMM}_{\min}}{\mathrm{TRMM}_{\max} - \mathrm{TRMM}_{\min}} \tag{4}$$

where TRMM, $\mathrm{TRMM}_{\max}$, and $\mathrm{TRMM}_{\min}$ are the values of precipitation, maximum precipitation, and minimum precipitation of each pixel, respectively, in the same month during the study period of 2000–2018. PCI changes from 0 to 1, and the corresponding precipitation changes from extremely low to highest.

5) SMCI: Agricultural drought can be characterized by soil moisture, and SMCI is an index that characterizes soil information [40]. SMCI is defined as follows:

$$\mathrm{SMCI} = \frac{\mathrm{SM} - \mathrm{SM}_{\min}}{\mathrm{SM}_{\max} - \mathrm{SM}_{\min}} \tag{5}$$

where SM, $\mathrm{SM}_{\max}$, and $\mathrm{SM}_{\min}$ are the values of SM, maximum SM, and minimum SM of each pixel, respectively, in the same month during the study period of 2000–2018. The SMCI changes from 0 to 1, which corresponds to the change from extremely low to high.

6) FCI: SIF can reflect changes in photosynthesis. When drought occurs, soil water supply cannot meet the water requirements of crops. SIF can be used to characterize the response of plants to leaf and canopy water content [41], [42], and it is closely related to the photosynthesis of vegetation [43], [44]. The research of SIF and its changes can be used to monitor crop growth and agricultural drought, while there are few studies using SIF data as an indicator to construct a model [45]–[47]. FCI is defined as follows:

$$\mathrm{FCI} = \frac{\mathrm{SIF} - \mathrm{SIF}_{\min}}{\mathrm{SIF}_{\max} - \mathrm{SIF}_{\min}} \tag{6}$$

where SIF, $\mathrm{SIF}_{\max}$, and $\mathrm{SIF}_{\min}$ are the values of SIF, maximum SIF, and minimum SIF of each pixel, respectively, in the same month during the study period of 2000–2018.

The FCI changes from 0 to 1, and the corresponding crop conditions change from extremely low to optimal. In extreme drought conditions, FCI is close or equal to 0; under optimal crop coverage conditions, it is close to 1.

B. Principal Component Analysis

PCA is a statistical method that transforms a group of potentially correlated variables into uncorrelated ones through orthogonal transformation. The transformed group of variables is called principal components. The principle of PCA is to recombine the original variables into a new set of unrelated integrated ones. According to actual needs, a few sum variables can be taken out to reflect as much information on the original variables as possible [48]. The PCA process calculates the covariance matrix, eigenvalues, and eigenvectors among all input data. Then the percentage of the total variance of the dataset explained by each component is obtained. Finally, a series of new ones is calculated by multiplying the eigenvectors of the original input data [27], [49].

Although different drought monitoring indexes can monitor drought from the aspects of the atmosphere, soil, and crops, interrelated information among them exists. In addition, different drought monitoring indexes have various contributions to drought monitoring. Therefore, this study used the PCA method to extract the main information from VCI, TCI, PCI, ETCI, SMCI, and FCI. Then the redundant information is removed. In agricultural drought monitoring and assessment, VCI, TCI, PCI, SMCI, ETCI, and FCI can characterize drought in three aspects: atmosphere, soil, and crop. However, there exists interrelated information between them. In different crop growth stages, each index contributes differently to the characterization of agricultural drought. In this study, the monthly VCI, TCI, PCI, SMCI, ETCI, and FCI were calculated as input, and the same number of principal components bands were obtained through PCA method. Considering that the first principal component always contains more than 75% of the information from all indexes, this component is defined as a new drought index, that is, the CDMI.

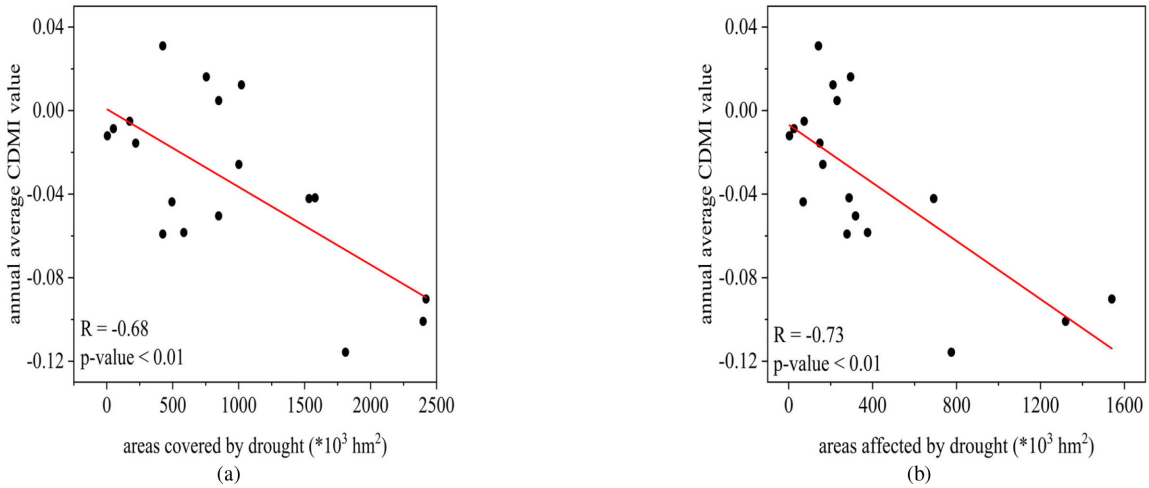

Fig. 3. Correlation between annual average CDMI value and areas covered and affected by drought. (a) Areas covered by drought. (b) Areas affected by drought.

C. Agricultural Drought Monitoring

To grasp the levels of agricultural drought, this study classified agricultural drought into four levels. The traditional threshold segmentation method was greatly affected by subjective experience, and the drought levels obtained by various indicators are quite different. This study averaged the CDMI pixel values of Henan Province from 2000 to 2018 and divided the comprehensive drought indicators into four levels (severe drought, moderate drought, light drought, and no drought) using the quantile thought to divide the threshold reasonably. This study used the CDMI to monitor the agricultural drought in Henan Province during the maize growing season (June to September). Based on the CDMI, the long-term agricultural drought was analyzed in Henan Province from 2000 to 2018, and the agricultural drought frequency was calculated from June to September.

IV. Results

A. Verification

To assess the accuracy of CDMI, this study used areas covered by drought, areas affected by drought and relative soil moisture for verification.

1) Verification Based on Drought Areas: The areas covered by drought and areas affected by drought were direct manifestations of agricultural drought. Especially the areas affected by drought was more closely related to drought. This study used the drought areas of Henan Province downloaded from the National Bureau of Statistics. This study selected data from 2000 to 2014 and 2014 to 2018 due to the lack of drought areas in 2015.

The annual average CDMI values from 2000 to 2018 were obtained by averaging the CDMI pixel values of agricultural areas from June to September. Fig. 3 shows the correlation between annual average CDMI value and areas covered and affected by drought. The results indicated that the annual average CDMI had negative correlations with areas covered and affected by drought. The correlation coefficients were –0.68 and –0.73.

2) Verification Based on Relative Soil Moisture: Relative soil moisture refers to the percentage of the soil moisture content to field water holding capacity. Agricultural drought is characterized by soil moisture. This section verified the accuracy of CDMI based on relative soil moisture data of the site to verify the ability of CDMI in monitoring agricultural drought. The Chinese Meteorological Data Network released a 10-day dataset of relative soil moisture (1991–2009). Given the timeliness and the lack of data, this study selected the site data from 2000 to 2009 as verification (see Fig. 4). Table I illustrates the specific site name, longitude, and latitude. The correlation coefficients between CDMI values and relative soil moisture were calculated simultaneously (see Fig. 4). The CDMI value had a positive correlation between relative soil moistures, and the correlation coefficients were between 0.37 and 0.91. The maximum correlation coefficient (R) was 0.91 (Neixiang site). The results showed that the CDMI value had high correlations with relative soil moisture, which could reflect the change of soil moisture. The CDMI could be feasibly used for agricultural drought monitoring in Henan Province.

B. Correlation Analysis With Crop Yield

Although there are many factors that can affect the changes of crop yield, agricultural drought is one of the main and direct factors leading to crop yield reduction. In Henan Province, summer maize is the main crop and the growth cycle of this crop is from June to September. In this section, to further explore the possible use of CDMI, the response of agricultural drought to summer maize yield was analyzed.

The CDMI was averaged by pixel from June to September in agricultural areas of Henan Province, and this value was regarded as the average CDMI for this year. Fig. 5 illustrates the correlation between the average CDMI value and yield from 2000 to 2018. In Henan Province, the CDMI had a positive correlation with the maize yield ($R = 0.52$) and the scattered points showed statistically significant correlation (p-value $<$ 0.01).

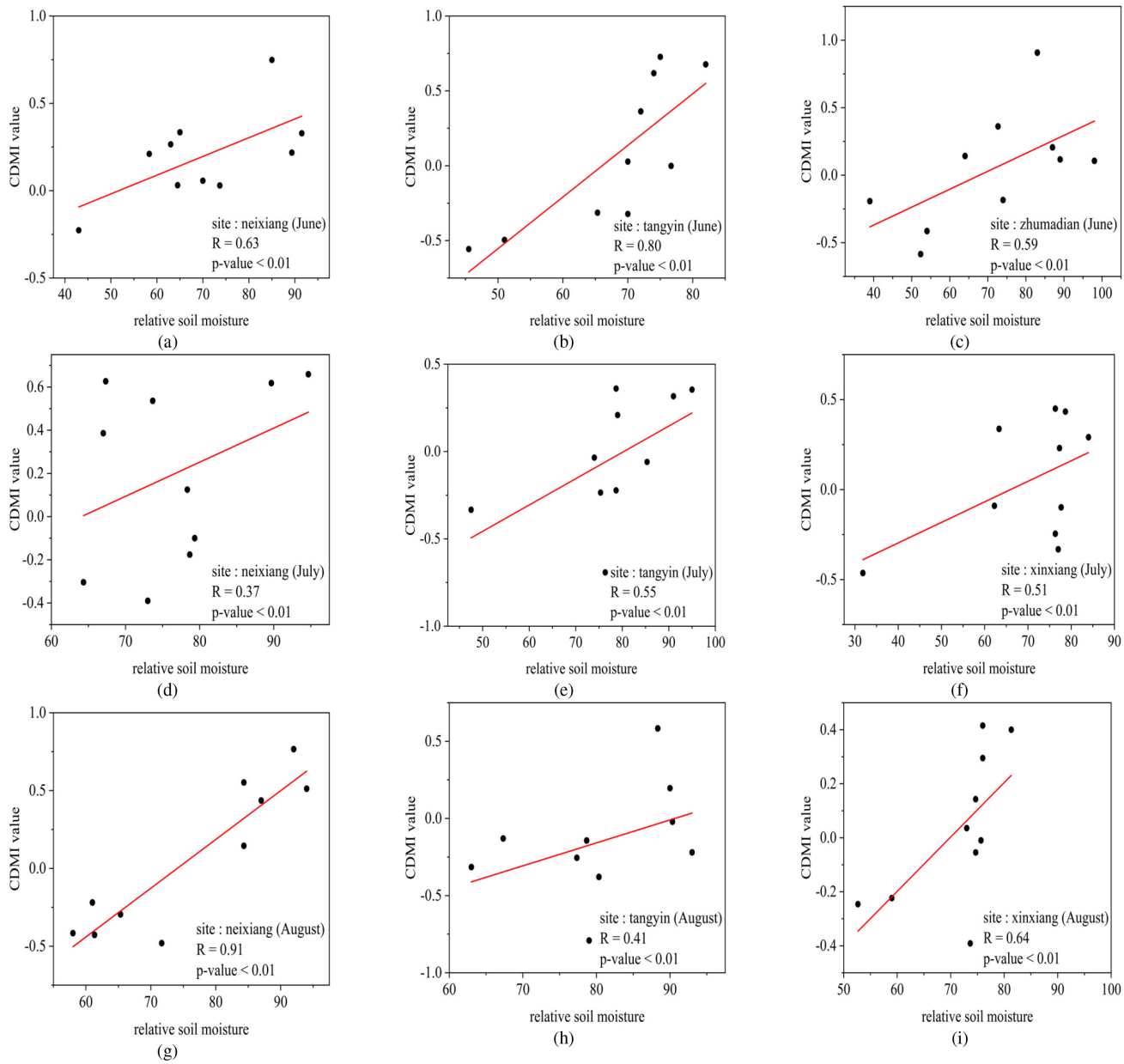

Fig. 4. Correlation between CDMI value and relative soil moisture. (a) Neixiang (June). (b) Tangyin (June). (c) Zhumadian (June). (d) Neixiang (July). (e) Tangyin (July). (f) Xinxiang (July). (g) Neixiang (August). (h) Tangyin (August). (i) Xinxiang (August).

TABLE I
SITE-BASED RELATIVE SOIL MOISTURE DATA AND CORRELATION COEFFICIENT WITH CDMI VALUE

time (2003-2009)	site name	longitude (°)	latitude (°)	correlation coefficient (R)
June	neixiang	111.86	33.05	0.63
	tangyin	114.35	35.93	0.80
	zhumadian	114.02	33.00	0.59
July	neixiang	111.86	33.05	0.37
	tangyin	114.35	35.93	0.55
	xinxiang	113.88	35.31	0.51
August	neixiang	111.86	33.05	0.91
	tangyin	114.35	35.93	0.41
	xinxiang	113.88	35.31	0.64

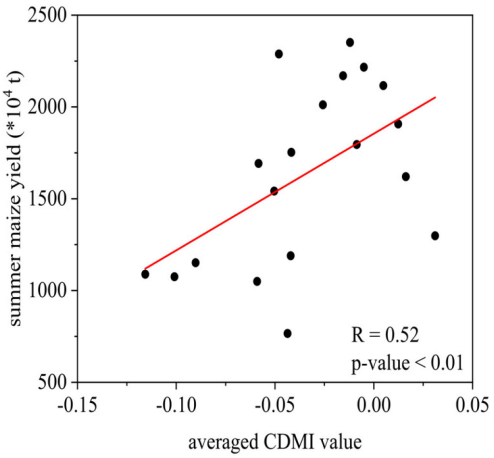

Fig. 5. Correlation between average CDMI value and maize yield.

C. Long-Term Agricultural Drought Monitoring Based on CDMI

A total of 76 agricultural drought distribution maps were obtained based on CDMI. This study calculated the monthly CDMI value during the maize growing season in Henan Province from 2000 to 2018 by averaging all pixel values in agricultural areas. The regional average CDMI values were sorted from small to large, and the quartiles (–0.1, –0.03, and 0.04) were selected as the dividing points of the drought levels. Meanwhile, based on the quartile method, agricultural drought was divided into four grades, namely, severe drought (CDMI $\leq$ –0.1), moderate drought (–0.1 $<$ CDMI $\leq$ –0.03), mild drought (–0.03 $<$ CDMI $\leq$ 0.04), and no drought (CDMI $>$ 0.04).

Fig. 6 shows the long-term CDMI value. The result showed that the CDMI could reflect the occurrence, duration, and severity of the agricultural drought. Severe drought occurred during the maize growing season in Henan Province in 2014 (the lowest average CDMI value, average CDMI = –0.116). The agricultural drought months were concentrated in July and August, which was consistent with the historical drought survey in agricultural areas.

D. Characteristic Year Agricultural Drought Monitoring Based on CDMI

According to long-term CDMI values (see Fig. 6), the result highlighted the agricultural drought in 2014. Particularly, the CDMI values reached extremely low levels in July and August (CDMI = –0.14, –0.22). Considering that June to August was the critical period for the growth of summer maize, a large amount of soil moisture was required for crop growth. If the soil water supply was insufficient, the agricultural drought will likely occur. Fig. 7 displays the spatial distribution of agricultural drought in July and August in Henan Province. The white areas in Henan Province were non-agricultural areas, and this part was not our research regions (see Fig. 1). The distribution maps illustrated that the drought in Henan Province was very serious in July. Exception for southeast (Xinyang), the southwest (Nanyang), and the north (Anyang, Puyang), the rest of the regions experienced severe agricultural droughts. In August, the drought areas expanded further, except for the Southeast (Xinyang) area, where severe agricultural droughts appeared in other regions.

E. Changes in Meteorological, Soil, and Crop

Agricultural drought is caused by the mutual influence of the atmosphere, soil, and crops. Changes in precipitation will cause changes in soil moisture, which will affect the growth of crops. SPEI, soil moisture, and NDVI were selected to characterize the changes in the atmosphere, soil, and crop, respectively. Long-term analysis of meteorological, soil, and crop was conducted by calculating annual average values during the maize growing season in agricultural areas (see Fig. 8). The results showed that SPEI, NDVI, and CDMI have similar fluctuations. SPEI, NDVI, and CDMI had low inflection points in 2004, 2006, 2008, and 2014. In these years, the precipitation was relatively low, and agricultural droughts affected crop growth. Meanwhile, combined with soil moisture, the lowest value was in 2014, which also verified that the soil moisture in Henan Province was low during the summer maize growth period in 2014, which resulted in agricultural drought. However, compared with other indexes, the regional average soil moisture value did not show consistent fluctuations. In this study, the soil moisture data used was microwave soil moisture data product (ESA CCI), which only characterized the changes in surface moisture of soil. In agricultural areas of Henan Province, irrigation was always an important way to supply water to the soil. The part of irrigation could not be monitored, and soil moisture curve appeared inconsistent fluctuation.

F. Agricultural Drought Frequency

Drought frequency refers to the number of drought events. This section analyzed the frequency of different levels of agricultural drought. The spatial distribution of drought frequency (0–0.2, 0.2–0.4, 0.4–0.6, 0.6–0.8, 0.8–1) in agricultural areas was determined using the drought maps from 2000 to 2018. The drought frequency of different drought severity levels from June to September was calculated (see Fig. 9). Moreover, the area proportions of each drought frequency under the influence of different droughts were also calculated (see Table II). The significant differences in the frequency of severe, moderate, and mild droughts were analyzed.

V. Discussion

A. Analysis of Verification Results

The CDMI had a positive correlation with relative soil moisture, areas covered by drought, and areas affected by drought. The relative soil moisture was an intuitive manifestation of the soil moisture content, which directly affected the occurrence of agricultural drought. Furthermore, the areas affected by drought were more closely related to agricultural drought.

The CDMI and relative soil moisture had a very high positive correlation (maximum R was 0.91) (see Fig. 4). This study also used the statistical data in Henan Province from 2000 to

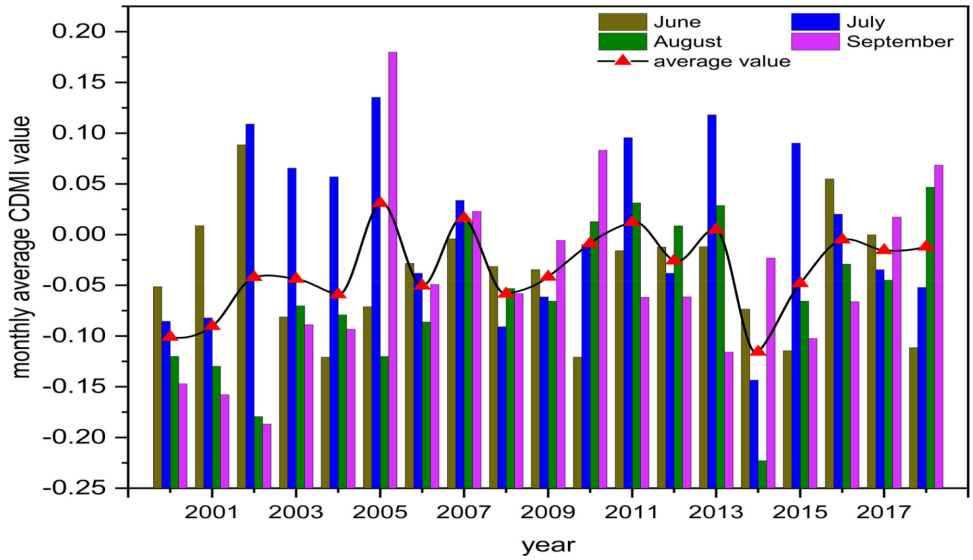

Fig. 6. Long-term CDMI value from 2000 to 2018.

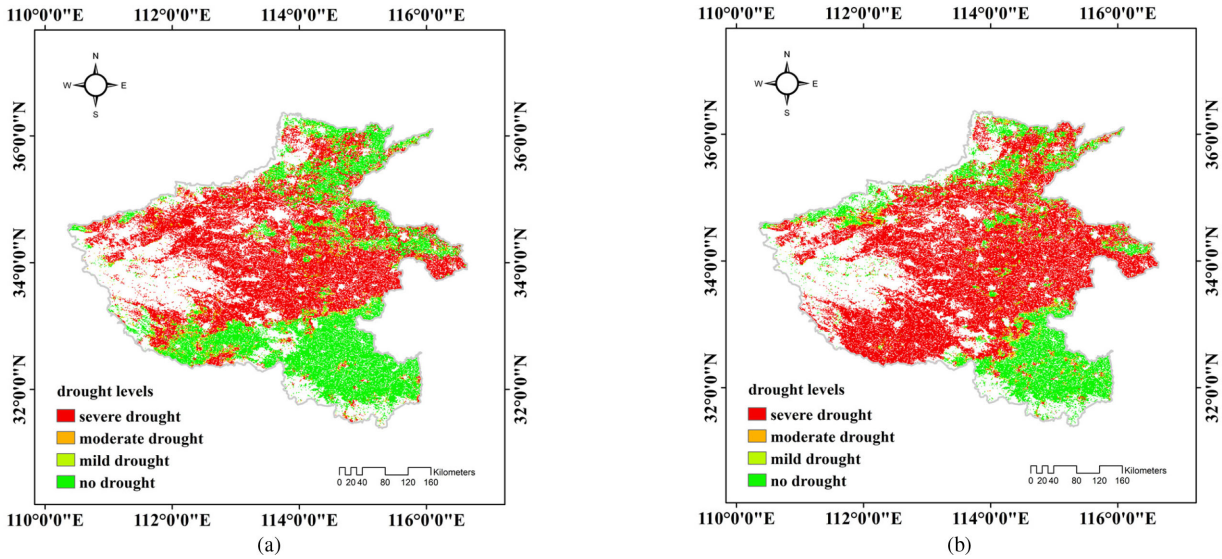

Fig. 7. Spatial distribution of agricultural drought in Henan Province 2014. (a) July. (b) August.

TABLE II
PROPORTION OF THE AGRICULTURAL AREAS OF EACH FREQUENCY UNDER DIFFERENT DROUGHT LEVELS

drought levels	month	0-0.2	0.2-0.4	0.4-0.6	0.6-0.8	0.8-1
severe drought	June	2.03%	30.32%	58.71%	8.91%	0.03%
	July	4.06%	43.66%	45.73%	6.49%	0.05%
	August	1.14%	24.14%	46.05%	27.74%	0.92%
	September	0.53%	30.26%	60.64%	8.57%	0.00%
moderate drought	June	92.32%	7.63%	0.05%	0.00%	0.00%
	July	90.89%	9.07%	0.03%	0.00%	0.00%
	August	91.26%	8.69%	0.05%	0.00%	0.00%
	September	90.47%	9.48%	0.05%	0.00%	0.00%
mild drought	June	90.62%	9.30%	0.08%	0.00%	0.00%
	July	90.37%	9.59%	0.04%	0.00%	0.00%
	August	91.70%	8.27%	0.03%	0.00%	0.00%
	September	88.81%	11.10%	0.09%	0.00%	0.00%

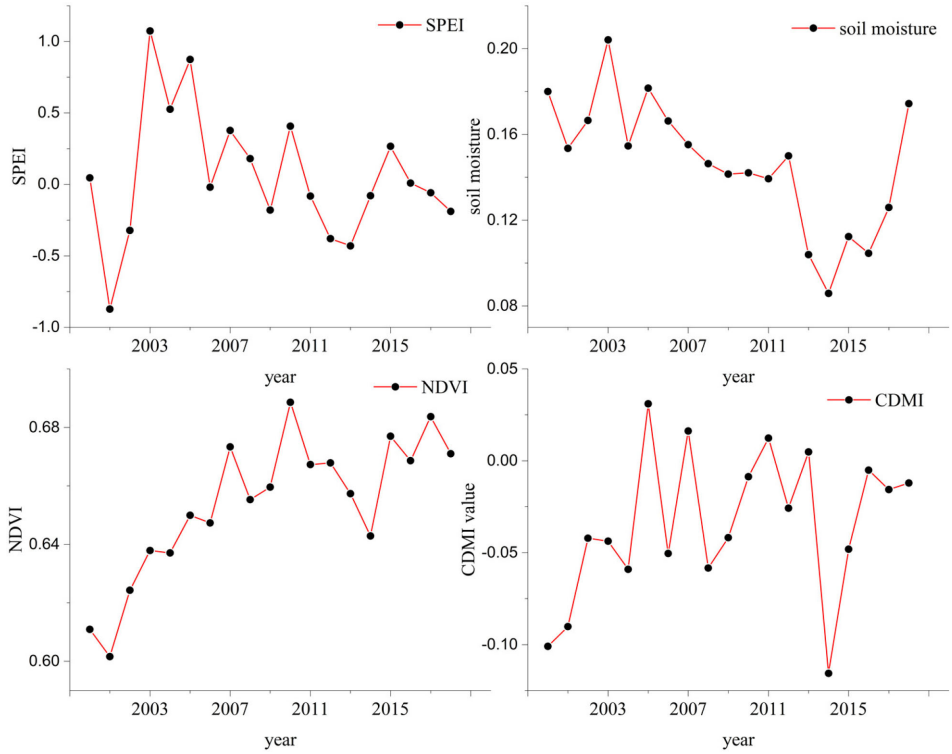

Fig. 8. Changes of SPEI, soil moisture, NDVI, and CDMI in agricultural areas.

2018 to verify the CDMI during the maize growing season (see Fig. 3). The annual average of VCI, TCI, SMCI, SPEI from June to September were calculated to evaluate the superiority of CDMI in monitoring agricultural drought. VCI can characterize changes in vegetation greenness. TCI and SMCI are proofs of the balance of water and heat in soil. SPEI can characterize meteorological factor. The correlations between areas affected by drought and annual VCI, TCI, SMCI, and SPEI were calculated (see Fig. 10). The correlation coefficients were –0.70, –0.37, –0.41, and –0.24, respectively. The results showed that the areas affected by drought had a higher correlation coefficient ($R = -0.73$) than other drought indexes. The occurrence of agricultural drought was the result of the combined action of a variety of drought-causing elements and the interaction of meteorological, soil, and crops. The CDMI was constructed through the PCA method, comprehensively considering a variety of factors that characterize agricultural drought. VCI, TCI, and SMCI only considered drought from a single factor. Therefore, the agricultural drought monitoring based on CDMI was more reliable and applicable.

B. Analysis of Agricultural Drought Results

From 2000 to 2018, during the summer maize growing season, Henan Province experienced severe agricultural drought in 2000, 2001, 2004, 2006, 2008, and 2014. Particularly in July and August of 2014, the monthly average CDMI value reached a very low level (CDMI = –0.14, –0.22).

The occurrence of agricultural droughts often starts with insufficient precipitation. Studies have shown that the agricultural drought had a lag effect of approximately one month on precipitation. Interannual variations of the anomalies of precipitation (June to August) and soil moisture (July to August) were calculated to analyze the relationship between agricultural drought and precipitation (see Fig. 11), and soil moisture (see Fig. 12) from 2003 to 2017. In June (2008, 2010–2014), July (2003, 2009, 2011–2015, 2017), and August (2006–2007, 2011–2017), the regional average precipitation values were lower than the multi-year average. In July (2009, 2011–2017) and August (2008–2010, 2012–2017), the regional average values of soil moisture were lower than the multi-year average. From June to August 2014, the precipitation below the mean conditions was particularly noticeable. The values of anomalies of precipitation were –46.33, –116.74, and –22.28. Specifically, in June and July, an anomaly of precipitation reached extremely low levels. Moreover, in the analysis, the anomaly of soil moisture (July and August) reached the lowest conditions (–0.07 and –0.09). Insufficient precipitation had caused a decrease in soil moisture, and soil water supply could not meet the water requirements of crops. Along with the crop's water shortage, agricultural drought also occurred.

C. Analysis of Agricultural Frequency

Results showed that the frequency of mild and moderate drought from June to September in most areas of Henan Province was less than 0.4, which was mainly concentrated in 0–0.2 (see Fig. 9). On the contrary, the frequency of severe drought in Henan Province was relatively high, and that in agricultural areas was higher than 0.4 (see Fig. 9). Table II illustrated the

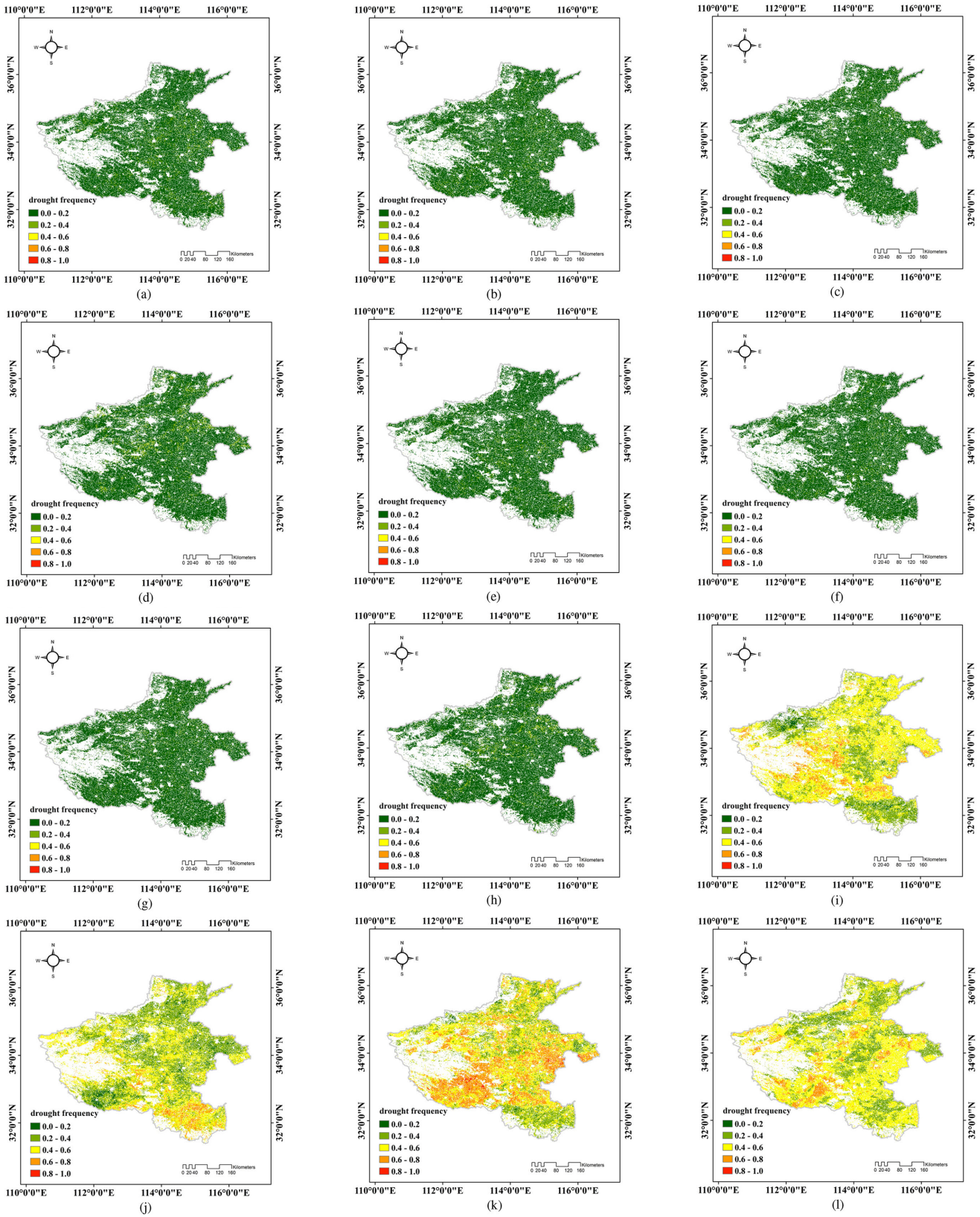

Fig. 9. Drought frequency of mild, moderate, and severe drought from June to September. (a) Mild drought (June). (b) Mild drought (July). (c) Mild drought (August). (d) Mild drought (September). (e) Moderate drought (June). (f) Moderate drought (July). (g) Moderate drought (August). (h) Moderate drought (September). (i) Severe drought (June). (j) Severe drought (July). (k) Severe drought (August). (l) Severe drought (September).

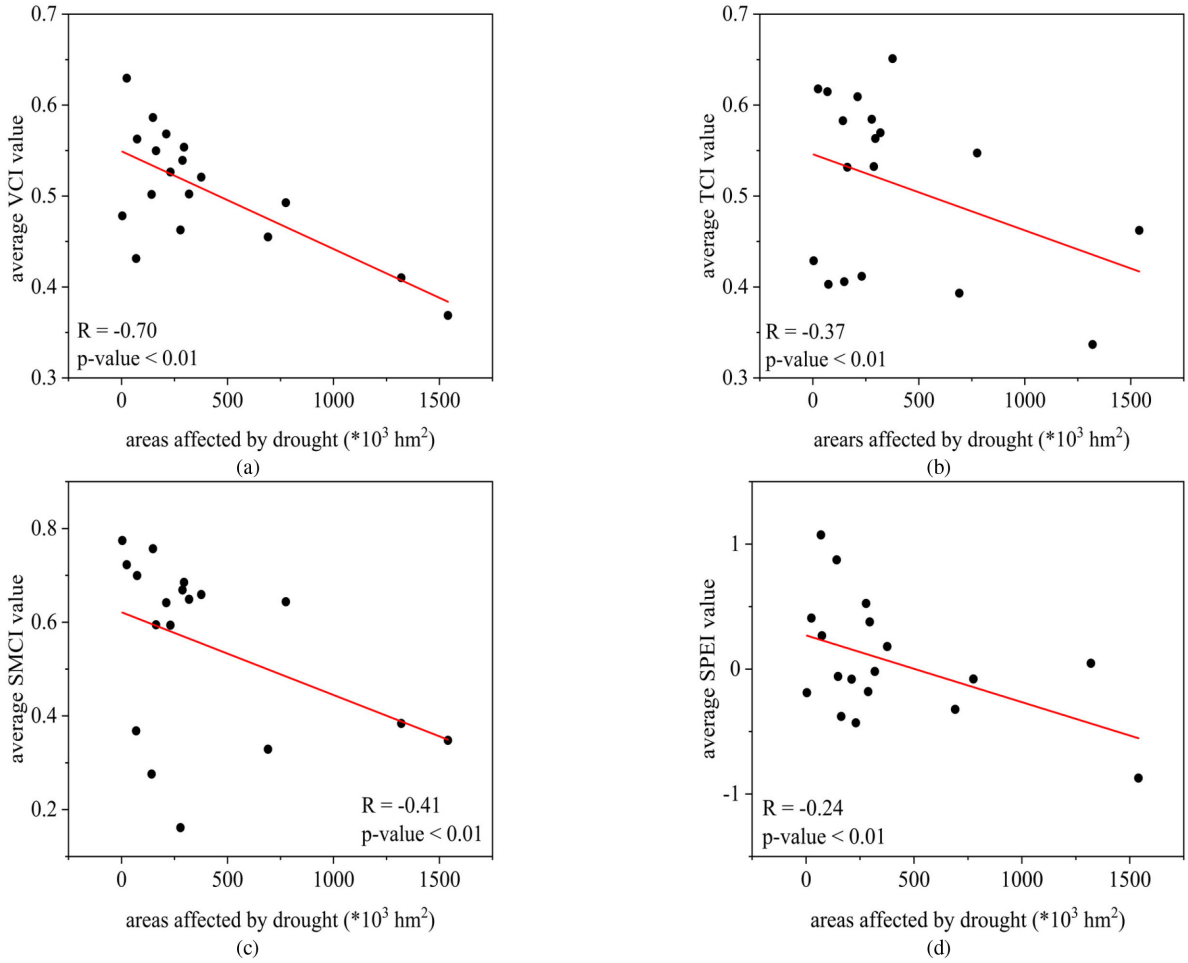

Fig. 10. Correlations between areas affected by drought and annual average VCI, TCI, SMCI, and SPEI. (a) VCI. (b) TCI. (c) SMCI. (d) SPEI.

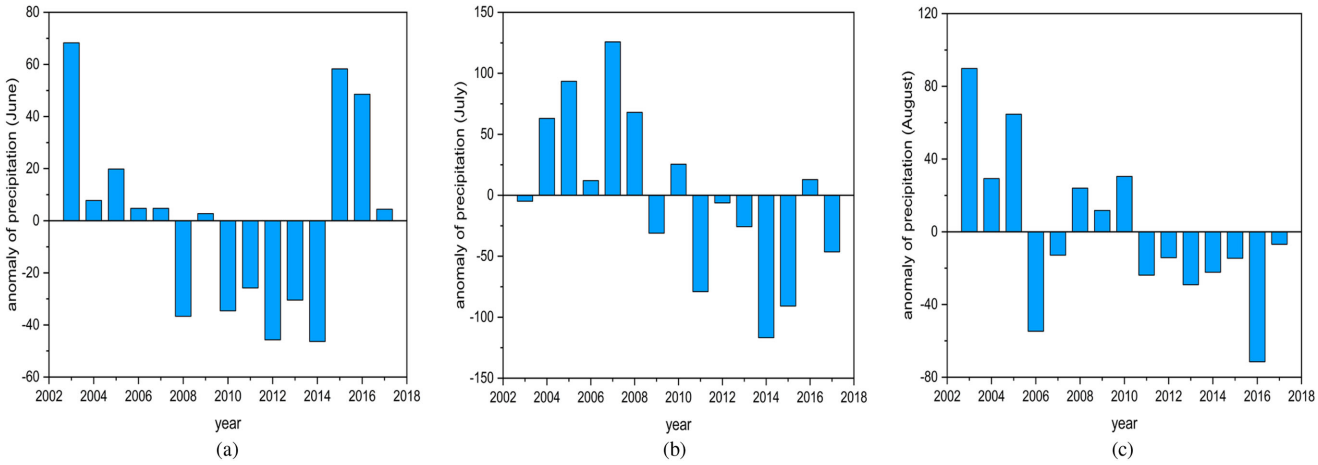

Fig. 11. Anomalies of precipitation from June to August. (a) June. (b) July. (c) August.

proportion of the area of each frequency under the influence of different droughts. For severe drought, the area ratios of the total agricultural area (more than 0.4) were 67.65% (June), 52.28% (July), 74.71% (August), and 69.20% (September) (see Table II). Particularly, the severe drought was highly significant in August because the maize in Henan Province in this month was in the ear stage (tasseling flowering) and pollen stage (spinning pollination and filling). At this time, the maize had undergone vegetative

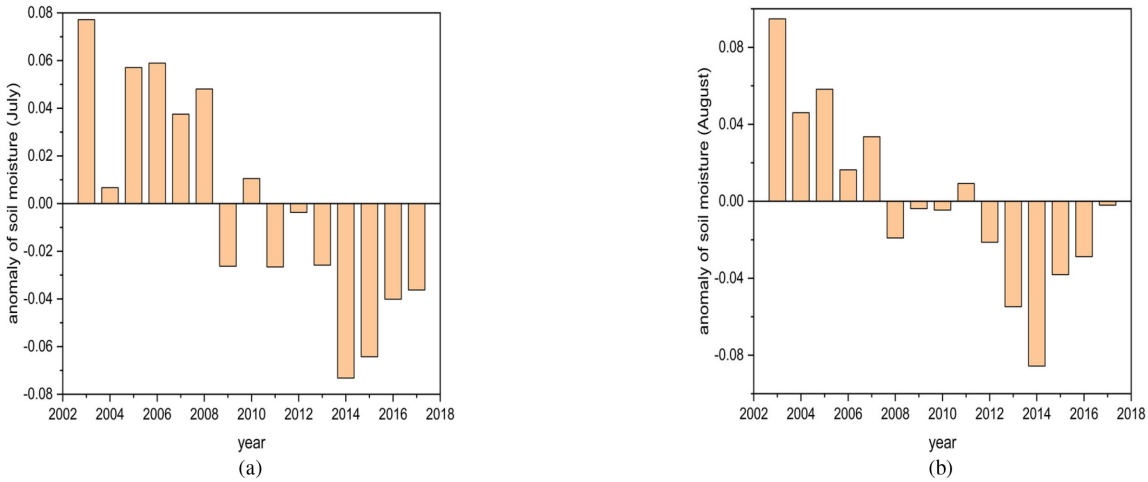

Fig. 12. Anomalies of soil moisture from July to August. (a) July. (b) August.

and reproductive growth, and its growth and development were vigorous. Without sufficient soil moisture as a supplement, drought is likely to occur.

In a severe drought, the central of Henan had a frequency of more than 0.4 in June, and the south-eastern of Henan also had greater than 0.4 in July. On the contrary, high-frequency areas increased significantly in August, with some areas in the south. The situation improved in September. The analysis of drought frequency showed that the frequency of severe drought was relatively high from 2000 to 2018. In addition, the frequency of different types of droughts in various months and regions was not the same.

D. Limitation of the CDMI

Agricultural drought is a complex and long-term phenomenon and it is caused by the interaction of multiple drought-causing factors. Agricultural drought does not have a linear relationship with drought-causing factors and there are correlations between them. In this study, PCA method was used to reduce redundancy of information and establish the CDMI. Several types of drought factors were considered including precipitation, vegetation index, land surface temperature, evapotranspiration, microwave soil moisture, and solar-induced chlorophyll fluorescence. Compared with other drought studies using PCA method [27], [50], more drought factors were considered from atmosphere, soil, and crops. For example, microwave soil moisture data, which could directly characterize changes in soil moisture content; and solar-induced chlorophyll fluorescence data, which could reflect the photosynthesis of crops and were more conducive to early drought monitoring. However, there were still some limitations.

1) This study calculated the agricultural drought in Henan Province based on the CDMI. The new index (CDMI) was applicable to the agricultural drought monitoring and assessment during the summer maize growing season in Henan Province. The research crop was corn. However, winter wheat is still the main crop in Henan Province. Hence, the applicability of the CDMI for different varieties of crops in regions is worth studying.
2) In this study, the time scale was based on monthly results. The occurrence of agricultural drought is a long-term and continuous process. In different times of one month, the intensity of agricultural drought can be different. A study of drought changes based on 10–15 days is necessary.
3) This study considered varies of agricultural drought factors. However, the impact of human activities on drought should not be ignored, especially irrigation. The effect of irrigation on the results is not considered in this study. Therefore, future research can integrate irrigation data in comprehensive drought monitoring.

VI. Conclusion

This study comprehensively considered the atmosphere (precipitation), soil (soil moisture, land surface temperature), and crops (vegetation index, evapotranspiration, and chlorophyll fluorescence). Moreover, the study selected VCI, TCI, PCI, SMCI, ETCI, and FCI as input through the PCA method to construct a new index called the CDMI. The CDMI had a positive correlation with relative soil moisture, and the correlation coefficient (R) were between 0.37 and 0.91. The annual average CDMI value had a negative correlation with areas covered by drought and areas affected by drought. The correlation coefficients (R) were –0.68 and –0.73. The CDMI was applied to the agricultural drought monitoring in Henan Province, combined with the changes of SPEI, SM, and NDVI to analyze the changes of agricultural drought in Henan Province. The results showed that the severe agricultural drought occurred in 2000, 2001, 2004, 2006, 2008, and 2014. Henan Province experienced severe agricultural drought in July and August 2014, which was consistent with the actual situation. This study calculated the frequency of different drought levels in agricultural areas from June to September from 2000 to 2018. Combined with the drought frequency maps, the frequency of severe drought in agricultural areas was more than 0.4. Agricultural areas with a severe drought frequency exceeding 0.4 accounted for 67.65% (June), 52.28% (July), 74.71% (August), and 69.20% (September). These findings showed that Henan Province was dominated by severe drought during the

maize growing season. These results also indicated that the CDMI was a useful and precise index to monitor and assess regional agricultural drought.

ACKNOWLEDGMENT

The authors would like to thank the MODIS, TRMM, AMSR-E/AMSR2 soil moisture products, evapotranspiration, and land-used products. Those products are available online for free. The authors would also like to thank Dr. J. Xiao and X. Li who provided GOSIF data for this article, and Zhangfeng who provided ET data.

REFERENCES

[1] N. S. Diffenbaugh, J. S. Pal, R. J. Trapp, and F. Giorgi, "Fine-scale processes regulate the response of extreme events to global climate change," *Proc. Nat. Acad. Sci.*, vol. 102, no. 44, pp. 15774–15778, 2005.

[2] J. Keyantash and J. A. Dracup, "The quantification of drought: An evaluation of drought indices," *Bull. Amer. Meteorological Soc.*, vol. 83, no. 8, pp. 1167–1180, 2002.

[3] I. Logar and J. C. van den Bergh, "Methods to assess costs of drought damages and policies for drought mitigation and adaptation: Review and recommendations," *Water Resour. Manage.*, vol. 27, no. 6, pp. 1707–1720, 2013.

[4] D. A. Wilhite, "Drought as a natural hazard: Concepts and definitions," *Droughts: Global Assessment. London: Routledge*, 2000.

[5] Z. Zhang, W. Xu, Q. Qin, and Z. Long, "Downscaling solar-induced chlorophyll fluorescence based on convolutional neural network method to monitor agricultural drought," *IEEE Trans. Geosci. Remote Sens.*, vol. 59, no. 2, pp. 1012–1028, Feb. 2021.

[6] M. Svoboda *et al.*, "The drought monitor," *Bull. Amer. Meteorological Soc.*, vol. 83, no. 8, pp. 1181–1190, 2002.

[7] A. Dai, "Drought under global warming: A review," *Wiley Interdiscipl. Rev., Climate Change*, vol. 2, no. 1, pp. 45–65, 2011.

[8] A. AghaKouchak *et al.*, "Remote sensing of drought: Progress, challenges and opportunities," *Rev. Geophys.*, vol. 53, no. 2, pp. 452–480, 2015.

[9] D. A. Wilhite and M. H. Glantz, "Understanding: The drought phenomenon: The role of definitions," *Water Int.*, vol. 10, no. 3, pp. 111–120, 1985.

[10] L. Zhang, W. Jiao, H. Zhang, C. Huang, and Q. Tong, "Studying drought phenomena in the continental United States in 2011 and 2012 using various drought indices," *Remote Sens. Environ.*, vol. 190, pp. 96–106, 2017.

[11] W. Jiao, C. Tian, Q. Chang, K. A. Novick, and L. Wang, "A new multi-sensor integrated index for drought monitoring," *Agricultural Forest Meteorol.*, vol. 268, pp. 74–85, 2019.

[12] H. West, N. Quinn, and M. Horswell, "Remote sensing for drought monitoring & impact assessment: Progress, past challenges and future opportunities," *Remote Sens. Environ.*, vol. 232, 2019, Art. no. 111291.

[13] T. B. McKee *et al.*, "The relationship of drought frequency and duration to time scales," in *Proc. 8th Conf. Appl. Climatol.*, 1993, vol. 17, pp. 179–183.

[14] W. C. Palmer, Meteorological Drought vol. 30, US Dept. Commerce, Weather Bureau, Washington, DC, USA, 1965.

[15] S. M. Vicente-Serrano, S. Beguería, and J. I. López-Moreno, "A multiscalar drought index sensitive to global warming: The standardized precipitation evapotranspiration index," *J. Climate*, vol. 23, no. 7, pp. 1696–1718, 2010.

[16] S. Park, J. Im, E. Jang, and J. Rhee, "Drought assessment and monitoring through blending of multi-sensor indices using machine learning approaches for different climate regions," *Agricultural Forest Meteorol.*, vol. 216, pp. 157–169, 2016.

[17] S. Park, J. Im, S. Park, and J. Rhee, "Drought monitoring using high resolution soil moisture through multi-sensor satellite data fusion over the Korean peninsula," *Agricultural Forest Meteorol.*, vol. 237, pp. 257–269, 2017.

[18] X. Zhou *et al.*, "Drought monitoring using the Sentinel-3-based multiyear vegetation temperature condition index in the Guanzhong plain, China," *IEEE J. Sel. Topics Appl. Earth Observ. Remote Sens.*, vol. 13, pp. 129–142, Dec. 3, 2019.

[19] J. Rouse, R. Haas, J. Schell, and D. Deering, "Monitoring vegetation systems in the great plains with ERTS," in *Proc. 3rd Earth Resour. Technol. Satellite-1 Symp.*, 1974, pp. 301–317.

[20] L. Yang, B. K. Wylie, L. L. Tieszen, and B. C. Reed, "An analysis of relationships among climate forcing and time-integrated NDVI of grasslands over the US northern and central great plains," *Remote Sens. Environ.*, vol. 65, no. 1, pp. 25–37, 1998.

[21] F. N. Kogan, "Droughts of the late 1980s in the united states as derived from NOAA Polar-orbiting satellite data," *Bull. Amer. Meteorological Soc.*, vol. 76, no. 5, pp. 655–668, May 1995.

[22] F. N. Kogan, "Application of vegetation index and brightness temperature for drought detection," *Adv. Space Res.*, vol. 15, no. 11, pp. 91–100, 1995.

[23] F. N. Kogan, "Global drought watch from space," *Bull. Amer. Meteorological Soc.*, vol. 78, no. 4, pp. 621–636, Apr. 1997.

[24] J. Rhee, J. Im, and G. J. Carbone, "Monitoring agricultural drought for arid and humid regions using multi-sensor remote sensing data," *Remote Sens. Environ.*, vol. 114, no. 12, pp. 2875–2887, 2010.

[25] A. Zhang and G. Jia, "Monitoring meteorological drought in semiarid regions using multi-sensor microwave remote sensing data," *Remote Sens. Environ.*, vol. 134, pp. 12–23, 2013.

[26] A. Karnieli, M. Bayasgalan, Y. Bayarjargal, N. Agam, S. Khudulmur, and C. Tucker, "Comments on the use of the vegetation health index over Mongolia," *Int. J. Remote Sens.*, vol. 27, no. 10, pp. 2017–2024, 2006.

[27] L. Du *et al.*, "A comprehensive drought monitoring method integrating MODIS and TRMM data," *Int. J. Appl. Earth Obs. Geoinf.*, vol. 23, pp. 245–253, 2013.

[28] C. Hao, J. Zhang, and F. Yao, "Combination of multi-sensor remote sensing data for drought monitoring over Southwest China," *Int. J. Appl. Earth Obs. Geoinf.*, vol. 35, pp. 270–283, 2015.

[29] A. K. Mishra and V. P. Singh, "A review of drought concepts," *J. Hydrol.*, vol. 391, nos. 1/2, pp. 202–216, 2010.

[30] R. L. Hanson, "Evapotranspiration and droughts," Compilers, National Water Summary 1988-89–Hydrologic Events and Floods and Droughts US Geological Surv. Water-Supply Paper, 2375, 1991, pp. 99–104.

[31] C. A. Jaleel *et al.*, "Drought stress in plants: A review on morphological characteristics and pigments composition," *Int. J. Agric. Biol*, vol. 11, no. 1, pp. 100–105, 2009.

[32] Y. Li, W. Ye, M. Wang, and X. Yan, "Climate change and drought: A risk assessment of crop-yield impacts," *Climate Res.*, vol. 39, no. 1, pp. 31–46, 2009.

[33] Y. Cao and H. Wei, "Spatio-temporal characteristics of adaptability between crop water requirements for summer maize and rainfall in Henan province, China," *Environ. Sci. Pollut. Res.*, vol. 27, pp. 37419–37431, 2020.

[34] G. B. Senay, S. Bohms, and J. P. Verdin, "Remote sensing of evapotranspiration for operational drought monitoring using principles of water and energy balance," *Environ. Sci.*, 2012.

[35] X. Li and J. Xiao, "A global, 0.05-degree product of solar-induced chlorophyll fluorescence derived from OCO-2, MODIS, and reanalysis data," *Remote Sens.*, vol. 11, no. 5, pp. 1–9, 2019.

[36] Z. Xu *et al.*, "Trends in global vegetative drought from long-term satellite remote sensing data," *IEEE J. Sel. Topics Appl. Earth Observ. Remote Sens.*, vol. 13, pp. 815–826, Feb. 10, 2020.

[37] M. Dikici and M. Aksel, "Evaluation of two vegetation indices (NDVI and VCI) over Asi basin in Turkey," *Teknik Dergi*, vol. 32, no. 4, pp. 1–17, 2020.

[38] R. G. Allen, M. Tasumi, and R. Trezza, "Satellite-based energy balance for mapping evapotranspiration with internalized calibration (METRIC)—Model," *J. Irrigation Drainage Eng.*, vol. 133, no. 4, pp. 380–394, 2007.

[39] Z. Li, Y. Han, and T. Hao, "Assessing the consistency of remotely sensed multiple drought indices for monitoring drought phenomena in continental China," *IEEE Trans. Geosci. Remote Sens.*, vol. 58, no. 8, pp. 5490–5502, Aug. 2020.

[40] Q. Liu, S. Zhang, H. Zhang, Y. Bai, and J. Zhang, "Monitoring drought using composite drought indices based on remote sensing," *Sci. Total Environ.*, vol. 711, 2020, Art. no. 134585.

[41] F. Daumard *et al.*, "A field platform for continuous measurement of canopy fluorescence," *IEEE Trans. Geosci. Remote Sens.*, vol. 48, no. 9, pp. 3358–3368, Sep. 2010.

[42] J. Grace, C. Nichol, M. Disney, P. Lewis, T. Quaife, and P. Bowyer, "Can we measure terrestrial photosynthesis from space directly, using spectral reflectance and fluorescence?," *Glob. Change Biol.*, vol. 13, no. 7, pp. 1484–1497, 2007.

[43] J. McFarlane *et al.*, "Plant stress detection by remote measurement of fluorescence," *Appl. Opt.*, vol. 19, no. 19, pp. 3287–3289, 1980.

[44] L. Guanter *et al.*, "Global and time-resolved monitoring of crop photosynthesis with chlorophyll fluorescence," *Proc. Nat. Acad. Sci.*, vol. 111, no. 14, pp. E1327–E1333, 2014.

[45] K. Guan *et al.*, "Improving the monitoring of crop productivity using spaceborne solar-induced fluorescence," *Glob. Change Biol.*, vol. 22, no. 2, pp. 716–726, 2016.
[46] S. Wang, C. Huang, L. Zhang, Y. Lin, Y. Cen, and T. Wu, "Monitoring and assessing the 2012 drought in the great plains: Analyzing satellite-retrieved solar-induced chlorophyll fluorescence, drought indices, and gross primary production," *Remote Sens.*, vol. 8, no. 2, p. 61, 2016.
[47] Z. Zhang, W. Xu, Y. Chen, and Q. Qin, "Monitoring and assessment of agricultural drought based on solar-induced chlorophyll fluorescence during growing season in north China plain," *IEEE J. Sel. Topics Appl. Earth Observ. Remote Sens.*, vol. 14, pp. 775–790, Oct. 21, 2020.
[48] A. Richards John and J. Xiuping, *Remote Sensing Digital Image Analysis: An Introduction*. Berlin, Germany: Springer-Verlag, 1999.
[49] R. Lasaponara, "On the use of principal component analysis (PCA) for evaluating interannual vegetation anomalies from SPOT/VEGETATION NDVI temporal series," *Ecological Model.*, vol. 194, no. 4, pp. 429–434, 2006.
[50] S. S. Kulkarni, B. D. Wardlow, Y. A. Bayissa, T. Tadesse, M. D. Svoboda, and S. S. Gedam, "Developing a remote sensing-based combined drought indicator approach for agricultural drought monitoring over Marathwada, India," *Remote Sens.*, vol. 12, no. 13, 2020, Art. no. 2091.

Zhaoxu Zhang was born in Hebei, China. He received the M.S. degree from China University of Geosciences (Beijing), Beijing, China, in 2016. He is currently working toward the Ph.D. degree with the School of Earth and Space Science, Peking University, Beijing.

His main research interests include agricultural drought monitoring and soil moisture retrieval.

Wei Xu was born in Anhui, China. He received the B.S. degree from Peking University, Beijing, China, in 2017. He is currently working toward the Ph.D. degree with the School of Earth and Space Science, Peking University.

His research interests include agricultural remote sensing, soil moisture retrieval, microwave remote sensing modeling, and machine learning in remote sensing.

Zhenwei Shi received B.S. and M.S. degrees in surveying and mapping from the China University of Geosciences, Beijing, China, in 2013 and 2016, respectively. He is currently working toward the Ph.D. degree in photogrammetry and remote sensing at Peking University.

His research interests include aerosol and cloud remote sensing and LiDAR remote sensing.

Qiming Qin received the B.S. degree in geography from Nanjing Normal University, Nanjing, China, in 1982, the M.S. degree in regional geography from Shaanxi Normal University, Xi'an, China, in 1987, and the Ph.D. degree in physical geography from Peking University, Beijing, China, in 1990.

From July 1990 to July 1992, he joined the Mathematical School, Peking University, for a Postdoctoral appointment. He is a Professor with the School of Earth and Space Sciences, Peking University, and Beijing Key Laboratory of spatial Information Integration and 3S engineering application. He also serves as the Director of Geographic Information System Technology Innovation Center of the Ministry of Natural Resources. His research interests include quantitative remote sensing and intelligent understanding of remote sensing image.